

Design and Performances of Multi-Tooth Stator Permanent Magnet Flux Switching Machine for Light Weight Applications

M. F. Omar^{1*}, E. Sulaiman^{2*}, L. I. Jusoh³, S. M. N. S. Othman⁴, S. A. L. S. Badrudden⁵

^{1,2,3,4,5} Research Center For Applied Electromagnetics (EMCenter), Faculty of Electrical and Electronic Engineering, Universiti Tun Hussein Onn Malaysia, 86400 Parit Raja, Johor, Malaysia.

*Corresponding authors E-mail: fairoz.omar@yahoo.com

Abstract

Permanent magnet flux switching machines (PMFMSs) in which their torque performance produced by interaction between armature coils and permanent magnet (PM) have been widely designed for various applications. In this regard, single-phase 8Slots-12Poles PMFMS with single tooth stator is considered the most suitable candidate for light weight applications because of their advantages of lower copper loss, high efficiency and robust rotor. However, issues of low torque performance due to weak flux linkage, high of PM volume, and high distortion in back-emf that need to be improved. In this paper, a new design of single-phase PMFMS using multi-tooth stator is proposed. Both PMFMSs have been designed using JMAG Designer version 15 and analysed through 2D-FEA. Parameters of stator outer radius, rotor outer radius, air gap, and stack length are set to 37.5mm, 22mm, 0.25mm, and 20.3mm, respectively. Based on the 2D-FEA, PM flux linkage and torque performances of the PMFMS using multi-tooth are 5 times and 38% higher than PMFMS using single-tooth. As a conclusion, single-phase 4Slot-12Poles PMFMS using multi-tooth stator considered as the best candidate for light weight applications due to the less PM volume, and good performances of torque, power and based speed of 1.44Nm, 219W, 1,062rpm, respectively.

Keywords: Flux Switching Machine; Light Weight Applications; Multi-Tooth Stator; Single-Phase; Permanent Magnet.

1. Introduction

Hybrid electric vehicles (HEV), using combination of an internal combustion engine (ICE) and one or more electric traction motors, are widely considered as the most promising green vehicles. As viable candidates of electric machines for HEV drives, there are several types of electric machines that synonym with HEV such as DC machines, and permanent magnet synchronous machines (PMSMs). DC machines should be widely accepted for electric vehicles (EV) and HEV drives because they can use a battery as a DC-supply as it is and have an advantage of simple control principle based on the orthogonal disposition of field and armature mmf. However, the essential problem of DC drives, which is caused by commutator and brush, makes them less reliable and unsuitable for a maintenance-free drives [1]-[2].

On the other hand, PMSMs, in particular Interior Permanent Magnet Synchronous Motors (IPMSMs) have had no commutator and brush and therefore, they have been most capable of competing with other motors for the electric propulsion of HEVs. IPMSMs have had many advantages in terms of lighter weight, smaller size, high torque and power densities, high efficiency and high reliability. One of examples of successfully developed IPMSM has been installed on LEXUS RX400h in 2005 [3]. This has been able to be proved by the historical progress in the power density of main traction motor installed on Toyota HEVs [4].

Besides, PMSMs and DC machines have also been used as a prime mover for light weight applications that require low torque and high speed performances such as electric bicycles [5]-[6]. The use of electric bicycles has been increasing in recent years due to their lower energy consumption and environmental friendly [7].

Other examples of electric motors used for electric bicycles are Multi-Flux Permanent Magnet (MFPM), and Switch Reluctance Motor (SRM) [8]-[9]. Nevertheless, problems such as low torque, low power, constraint of rare earth permanent magnet, and high noise have led many studies to find a new technology in improving the performance of electric motors.

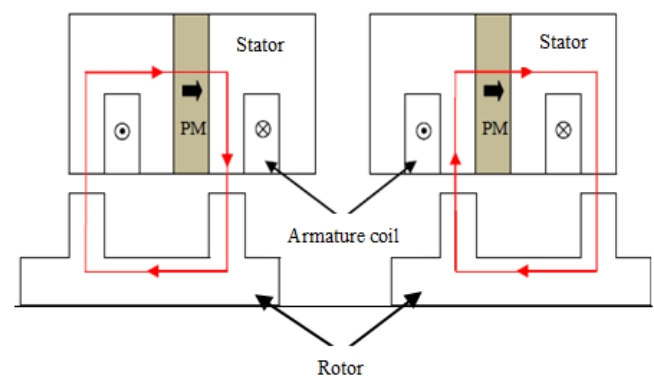


Fig. 1: Working principle of PMFMS

Therefore, as one of the effective approaches to increase the motor torque and power densities, permanent magnet flux switching machines (PMFMSs) is introduced. The working principle of the PMFMS is illustrated in Fig. 1. From the figure, the red arrows indicate the flux line of PM. The rotor pole aligns with one of two stator teeth over which a coil is wound. Then the permanent magnet (PM) flux linked in the coil stream from the stator and into the rotor pole. When the rotor moves forward to align with another stator tooth belonging to the same coil winding, the flux stream of the rotor pole and into the stator tooth. Thus, as the rotor moves, the flux linkage in the windings will change periodically [10]-[11]. In the previous design, a single-phase 8 Slots – 12 Poles (8S-12P) has been designed based on conventional inner rotor PMFMS using single tooth stator and salient rotor structure (PMFMS single-tooth) as shown in Fig. 2. Parameters of stator outer diameter, rotor outer diameter, stack length, and air gap are set to 75 mm and 22 mm, 20.3 mm and 0.25 mm, respectively. The 8S-12P PMFMS consists of 8 pieces of Neomax-35AH PM. These PM have been placed between in each armature coil windings and the weight of all PM is approximately 80g. In terms of performance, it can be concluded that the single phase 8S-12P PMFMS has been achieved the torque and power capabilities of 1.04 Nm and 674 W, respectively [12]. However, the single-phase 8S-12P PMFMS with single tooth stator structure can be improved due to low torque performance, high PM usage, and high back-emf distortion. In this research, a new single-phase PMFMS using multi-tooth stator structure is proposed. The proposed motor consists of 4 slots

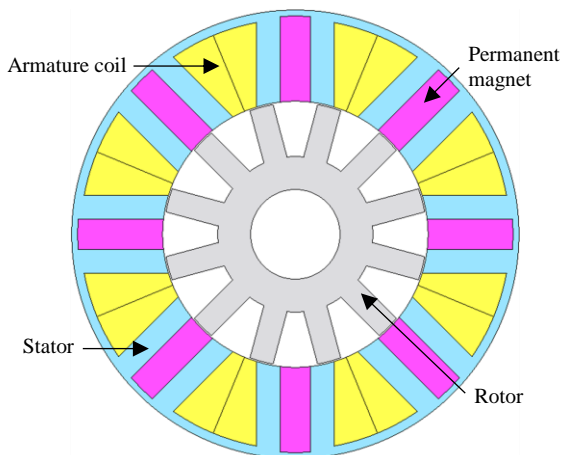


Fig. 2: The conventional PMFMS design using single tooth rotor.

for copper windings, 4 multi-tooth stator, 12 rotor poles and, 4 pieces of PM. 2D finite element analysis (2D-FEA) through JMAG Designer version 15 is used to analyse the flux linkage, flux distribution, flux line, back-emf, torque capability, and torque-power versus speed characteristics of the proposed motor.

2. Design Restrictions and Specifications of The Proposed PMFMS

The machine configurations of single-phase 4S-12P PMFMS using multi-tooth stator (PMFMS multi-tooth) is demonstrated in Fig. 3. From the figure, the armature coil windings are placed in between of PM, and alternate configuration. Each stator tooth has divided into 4 teeth. Table 1 shows the design specifications and parameters for the proposed machines. The split ratio of rotor outer diameter and stator outer diameter is set to 59% as standard motor design requirement. While, parameters of stator inner radius, air gap, stack length, and shaft radius are set to 22.25 mm, 0.25 mm, 20.3 mm, and 7.5 mm, respectively. Four pieces of PM with weight of 10.2 g is 8 times lighter than conventional PMFMS with single tooth stator. In short, equal stator back inner and stator pole

Table 1: Design restrictions, specifications and dimensions of the proposed 4S-12P PMFMS using multi-tooth stator

Items	Dimensions
Number of phase	1
No. of slots	4
No. of poles	12
Stator inner radius (mm)	22.25
Stator outer radius (mm)	37.5
Rotor outer radius (mm)	22
Rotor inner radius (mm)	7.5
Rotor tooth width (mm)	4
Stator pole height (mm)	15.25
Air gap (mm)	0.25
Stack length (mm)	20.3
Shaft radius (mm)	2.5
Magnet material	Neomax-35AH
Magnet mass (g)	10.2
Speed (rpm)	500
Armature current density, J_A (A_{rms}/mm^2)	10
Maximum current (A)	3.54
Number of turns armature coil	240

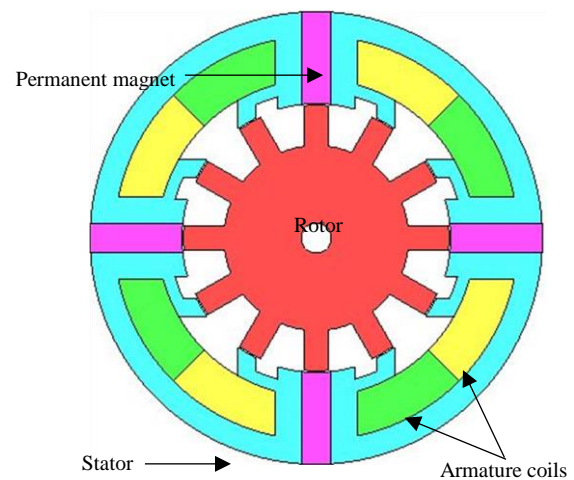


Fig. 3: Structure of the proposed PMFMS using multi-tooth

widths are predictable to allow flux stream from stator to rotor and vice versa smoothly with equal magnetic flux distribution. Design methodology of the proposed PMFMS using multi-tooth stator have three main sections in the implementation of this study: Geometry editor, JMAG designer and 2D-FEA testing. The Geometric editor and JMAG designer sections are the process of designing each motor structure and the internal setup of the proposed motors, respectively. Finally, the result performances of flux linkage, flux distribution, flux line, back-emf, various torque capability, and torque-power versus speed characteristics that have been investigated are analysed are presented.

3. 2D-FEA Performances of PMFMS using multi-tooth stator

3.1 Flux linkages

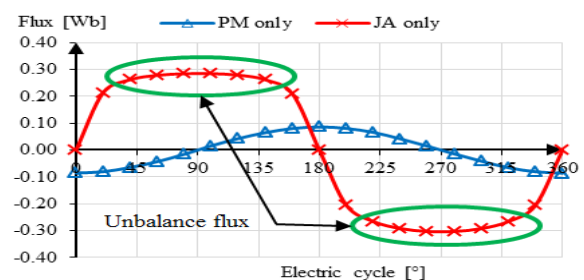
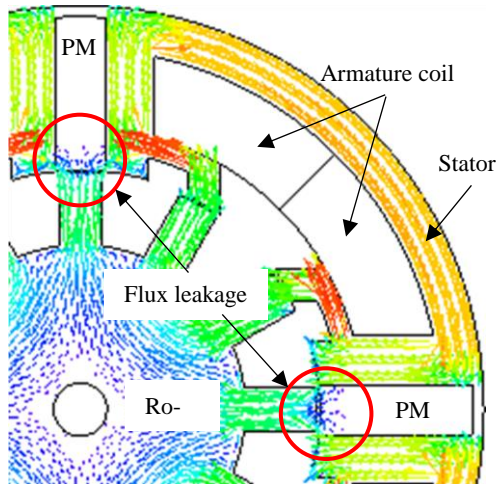
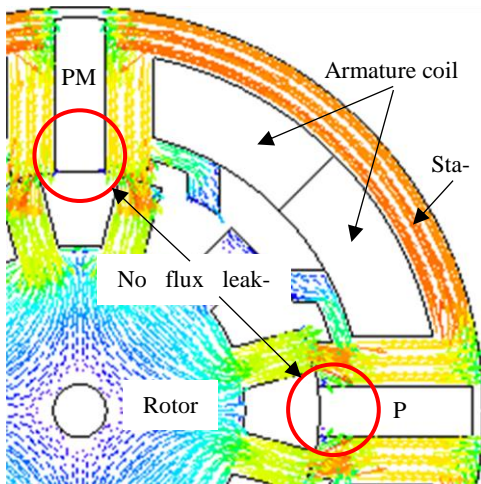


Fig. 4: Flux linkages of PMFMS using multi-tooth stator

Fig. 4 shows flux linkages of the proposed PMFSM using multi-tooth stator. Flux profile has been plotted in two conditions, initially when PM only and secondly, when J_A is set to a maximum of $10 \text{ A}_{\text{rms}}/\text{mm}^2$ without PM. Clearly, J_A flux linkage of 0.285 Wb is approximately 3 times higher than PM flux linkage. This clarifies that the flux linkage generated from PM is moved around the stator and rotor before arriving at armature coil winding. Besides, PM flux linkage lead 90° of J_A flux linkage, ensure the proposed motor is working based on standard operating principle of single-phase motor. However, the flux linkage of J_A only show unbalance between positive and negative cycles due to the flux leakage occurs between rotor and stator as illustrated in Fig. 5. Fig.



(a) Rotor at 90 degrees



(b) Rotor at 270 degrees

Fig. 5: Flux distributions of PMFSM multi-tooth

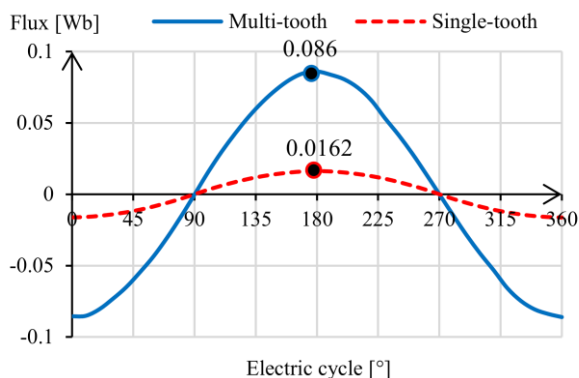


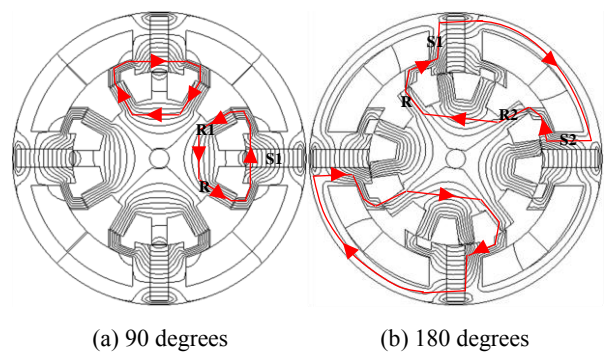
Fig. 6: Comparison of PM Flux linkage between PMFSM multi-tooth and PMFSM single-tooth.

5(a) shows the rotor at a 90° electric cycle, and flux leakage that has been occurred as marked in red cycle is due to the limited flux path between the rotor and the stator. Compared to flux linkage when rotor reach at 270° electric cycle as illustrated in Fig. 5(b), the flux path is wider, and it has facilitated flux flows, hence reducing the probability of flux leakage. In addition, PM flux linkage of 0.086 Wb has produced from the PMFSM multi-tooth is 5 times higher than PMFSM single-tooth design as illustrated in Fig. 6. This proves that the multi-tooth structure has facilitated flux stream from stator to rotor and vice versa, thus strengthening the flux linkage to form a complete cycle.

3.2 Flux Line

Fig. 7 shows the magnetic flux line generated by PM 90° and 180° electric cycles. Fig. 7 (a) illustrates the flux line when the rotor at 90° electric cycle. Obviously, the flux has flowed between a set of stator tooth and two rotor teeth, and flux attraction between rotor and stator at this point is zero. While, the highest flux attraction was recorded when the rotor at 180° electric cycles as demonstrated in Fig. 7 (b). From the figure, a complete cycle of flux has been generated through 2 sets of stator teeth and 2 rotor teeth and produces a high flux attraction.

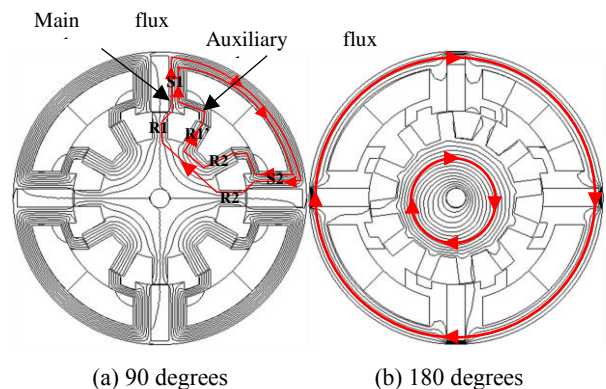
The flux line formed by maximum J_A of $10 \text{ A}_{\text{rms}}/\text{mm}^2$ of the proposed PMFSM multi-tooth is illustrated in Fig. 8. Fig. 8 (a) shows the flux line when the rotor at 90° electric cycle. From the diagram, a complete cycle of flux has been linked between 2 sets of stator teeth and 2 rotor teeth. Additionally, there is an auxiliary flux cycle with shorter flux path in the center of the main flux cycle, thus increasing the strength of flux linkage. Fig. 8(b) shows flux line when rotor at 180° electric cycle. From the figure, the flux linkage is zero because of flux does not legitimately flow from stator to rotor and vice versa to form a complete cycle of flux. In short, the flux line analyses have been proved the highest flux linkages of PM and J_A are achieved at 180° and 90° , respectively as discussed in sub-topic 3.1.



(a) 90 degrees

(b) 180 degrees

Fig. 7: Flux line of PM



(a) 90 degrees

(b) 180 degrees

Fig. 8: Flux line of armature current density, J_A

3.4 Back-emf Profile

Fig. 9 shows comparison of back-emf profile between the proposed PMFSM multi-tooth and PMFSM single-tooth. From the figure, the highest back-emf of 57.8 V and 11.8 V have been recorded

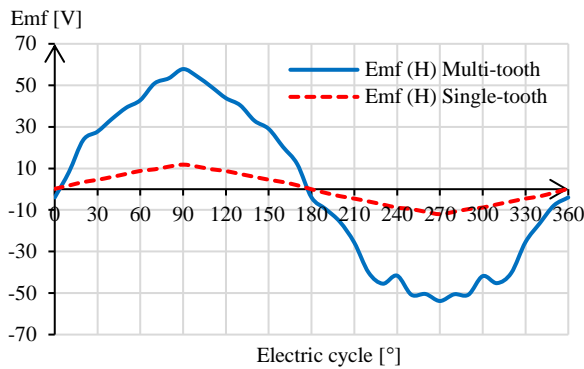


Fig. 9: Back-emf of PMFSM multi-tooth and PMFSM single-tooth.

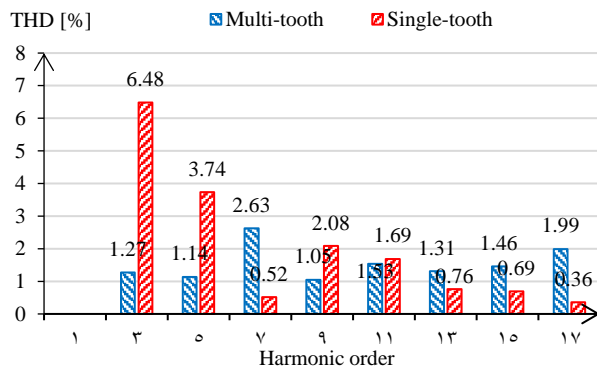


Fig. 10: THD versus harmonic order

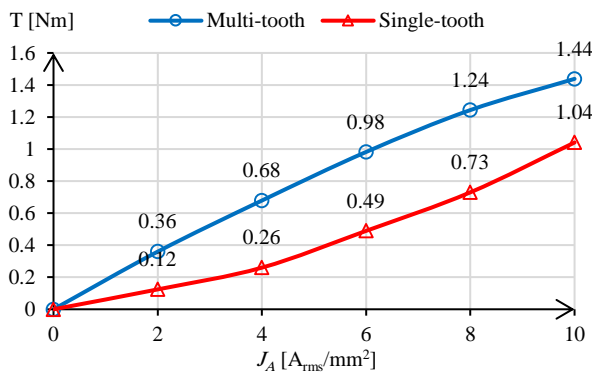


Fig. 11: Torque at various armature current densities, J_A of PMFSM multi-tooth and PMFSM single-tooth.

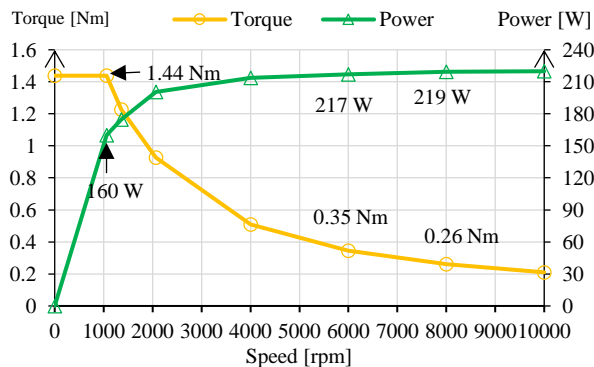


Fig. 12: Torque and power versus speed characteristics of PMFSM multi-tooth.

from PMFSM multi-tooth and PMFSM single-tooth, respectively. The back-emf of PMFSM single-tooth has been produced 5 times lower compared to the PMFSM multi-tooth due to the less PM flux linkage. Though back-emf of PMFSM multi-tooth is higher than PMFSM single-tooth, total harmonic distortion (THD) of PMFSM multi-tooth has a much lower than PMFSM single-tooth as shown in Fig. 10. Obviously, all THDs of PMFSM multi-tooth harmonic is below than 3%, only 7th harmonic indicates THD exceeds of 2%, and other harmonics have been recorded THD below 1.53%.

3.5 Torque at Various J_A

Torque capabilities of PMFSM multi-tooth and PMFSM single-tooth at various J_A are plotted in Fig. 11. Obviously, the torque increases parallelly with increase of J_A . At maximum J_A of 10 A_{rms}/mm^2 , the PMFSM multi-tooth design has produced torque of 1.44 Nm, 38% higher than PMFSM single-tooth design. It has proven that torque performance of PMFSM multi-tooth has been improved and suitable for light weight applications such as electric bicycles. From this analysis, it can be summarized that the higher flux linkage produced by multi-tooth stator structure has increased the flux strength, hence producing high torque.

3.6 Torque-Power Versus Speed Characteristics

The torque-power versus speed characteristics of the proposed PMFSM multi-tooth is demonstrated in Fig. 12. The investigation has been performed by diversifying J_A from 0 to 10 A_{rms}/mm^2 and varying armature current phase angle from 0° to 80°. Clearly, the highest torque of 1.44 Nm is obtained under based speed and power of 1,062 rpm and 160 W, respectively. While, the highest power of 219 W is achieved at speed of 8,000 rpm, and the corresponding torque is 0.26 Nm. Moreover, at the medium speed conditions of 4,000 rpm to 7,000 rpm, the corresponding torque is approximately 0.3 to 0.5 Nm, and the power capability is in the range of 210 W to 218 W.

4. Conclusions

A new design of single-phase PMFSM using multi-tooth stator structure has been presented. The procedure to design the proposed PMFSM multi-tooth has been clearly explained. The performance analyses of flux linkage, flux distribution, flux line, back-emf, torque capability at various armature current density, and torque-power versus speed characteristics have been investigated. Based on 2D-FEA, the proposed PMFSM multi-tooth has high PM flux linkage due to great characteristics of flux line and flux distribution.

The total weight for four pieces of PM is 10g, 8 times lighter than PMFSM single-tooth. In addition, harmonic interference to back-emf is also lower, in which all THDs are below 3%. As a conclusion, the proposed PMFSM using multi-tooth stator structure is considered as the best candidate for light weight applications due to the high initial performances of torque, power and based speed of 1.44 Nm, 219 W and 1,062 rpm, respectively.

Acknowledgement

This work was funded by Ministry of Education Malaysia (MOE) under FRGS Vot. 1651 grant thru Universiti Tun Hussein Onn Malaysia (UTHM).

References

[1] Chan CC, "The state of the art of electric, hybrid, and fuel cell vehicles", Proc. IEEE, Vol. 95, No. 4, (2007), pp. 704–718.

- [2] Emadi A, Lee YJ & Rajashekara K, "Power Electronics and Motor Drives in Electric, Hybrid Electric, and Plug-In Hybrid Electric Vehicles", *IEEE Trans. Ind. Electron.*, Vol. 55, No. 6, (2008), pp. 2237–2245.
- [3] Asano K, Inaguma Y, Ohtani H, Sato E, Okamura M & Sasaki S, "High Performance Motor Drive Technologies for Hybrid Vehicles", in *Fourth Power Conversion Conference-NAGOYA, PCC-NAGOYA*, (2007), pp. 1584–1589.
- [4] Sulaiman EB, Kosaka T & Matsui N, "Design study and experimental analysis of wound field flux switching motor for HEV applications", *Proc. - 2012 20th Int. Conf. Electr. Mach. ICEM 2012*, No. c, (2012), pp. 1269–1275.
- [5] Adnan A & Ishak D, "Finite element modeling and analysis of external rotor brushless DC motor for electric bicycle", in *2009 IEEE Student Conference on Research and Development (SCORED)*, (2009), pp. 376–379.
- [6] Yang Y, Rahman MM, Lambert T, Bilgin B & Emadi A, "Development of an External Rotor V-Shape Permanent Magnet Machine for E-Bike Application" *IEEE Trans. Energy Convers.*, Vol. PP, No. c, (2018), pp. 1–1.
- [7] Du W, Zhang D & Zhao X, "Research on battery to ride comfort of electric bicycle based on multi-body dynamics theory", in *Proceedings of the 2009 IEEE International Conference on Automation and Logistics (ICAL)*, (2009), pp. 1722–1726.
- [8] Seo JM, Rhyu SH, Jung IS & Jung HK, "A design of multi flux permanent-magnet machine for electric bicycles", in *Proceedings of the 2009 IEEE International Conference on Power Electronics-ECCE Asia*, (2015), pp. 1457–1461.
- [9] Lin J, Schofield N & Emadi A, "External-Rotor 6-10 Switched Reluctance Motor for an Electric Bicycle", *IEEE Trans. Transp. Electr.*, Vol. 1, No. 4, (2015), pp. 348–356.
- [10] Jenal M, Sulaiman E, Omar MF, Romalan GM & Soomro HA, "Development of a novel permanent magnet flux switching machine prototype for light weight electric vehicles", *2015 IEEE Student Conf. Res. Dev. (SCORED)*, (2015), pp. 739–744.
- [11] Jenal M, Sulaiman E, Ahmad MZ, Khan F & Omar MF, "A new alternate circumferential and radial flux (AlCiRaF) permanent magnet flux switching machine for light weight EV", *J. Magn.*, Vol. 21, No. 4, (2016), pp. 537–543.
- [12] Jusoh LI, Sulaiman E, Bahrim FS & Kumar R, "Design and Performance of 8Slot-12Pole Permanent Magnet Flux Switching Machines for Electric Bicycle Application Article", *Int. J. Power Electron. Drive Syst.*, Vol. 8, No. 1, (2017), pp. 248–254.